

Multipartite entanglement of random states of qubits

Giorgia Trotta,^{1,2,3} Paolo Scarafile,^{1,2,3} Paolo Facchi,^{2,3} Giuseppe Magnifico,^{2,3}
Angelo Mariano,⁴ Giorgio Parisi,^{5,6,7} Saverio Pascazio,^{2,3} and Karol Życzkowski^{8,9}

¹*Dipartimento di Fisica, Università di Napoli Federico II*

²*Dipartimento di Fisica, Università di Bari, 70126 Bari, Italy*

³*INFN, Sezione di Bari, 70125 Bari, Italy*

⁴*Energy Technologies and Renewable Sources Department,
ICT Division, ENEA (National Agency for New Technologies,
Energy and Sustainable Economic Development), 70125 Bari, Italy*

⁵*Dipartimento di Fisica, Università degli Studi di Roma La Sapienza*

⁶*Istituto Nazionale di Fisica Nucleare, Sezione di Roma I*

⁷*Institute of Nanotechnology (NANOTEC) - CNR, Rome unit*

⁸*Institute of Theoretical Physics, Faculty of Physics,*

Astronomy and Applied Computer Science, Jagiellonian University, Kraków, Poland

⁹*Center for Theoretical Physics (CFT), Polish Academy of Sciences, Warszawa, Poland*

We investigate multipartite entanglement via the statistical properties of pure quantum states of n -qubits. By analyzing the distribution of purity among balanced bipartitions, we compare Haar-typical states, uniformly distributed on the unit sphere of states, with Hadamard states, being characterized by equal weights in the computational basis. We analyze different ensembles of Hadamard states characterized by their phase distributions. Through analytical and numerical calculations, we show that Hadamard states exhibit, on average, a higher degree of entanglement than Haar-typical states. In addition, we show that a particular class of Hadamard states, characterized by real coefficients with alternating signs, known as hypergraph states, appears especially relevant in the search for maximally multipartite entangled states, both for their structural simplicity and the increased likelihood of sampling highly entangled states. These results identify Hadamard states as a tractable yet promising class for exploring multipartite entanglement structures and advancing the characterization of maximally multipartite entangled quantum states.

I. INTRODUCTION

Entanglement is a fundamental feature of quantum mechanics and a central resource in quantum information, enabling relevant applications such as quantum teleportation [1–3], quantum computation [4], quantum communication [5] and quantum cryptography [6–9]. While the bipartite entanglement of pure states is unambiguously quantified in terms of the entropy of either single-party reduced state [10–12], the quantification of multipartite entanglement remains more intricate and less unified [13–15]. This has led to multiple approaches being developed, each focusing on different aspects of the problem, for instance the invariance under permutation of the parties [16, 17], the scalability of the measure with the system size [18], the structural analogy with the bipartite von Neumann entropy [13] or the mutual exclusivity of single-partite and bipartite properties of subsystems [19]. These different characterizations of multipartite entanglement often yield distinct and, in some cases, incompatible classifications.

Various studies have shown that multipartite entanglement exhibits frustration, i.e., the impossibility of simultaneously maximizing entanglement across all bipartitions [20–24], making statistical methods from complex systems particularly suitable for its characterization.

In this context, analyzing the statistical distribution of entanglement measures, such as the purity over all balanced bipartitions and related quantities like the av-

erage linear entropy [13, 22, 25], has emerged as a powerful tool for characterizing multipartite entanglement [26]. This approach has been effectively applied to typical pure states sampled according to the Haar measure in qubit systems [27–30].

A particularly significant class of states is that of maximally multipartite entangled states (MMES), which are defined as those that maximize entanglement across all balanced bipartitions [25]. The presence of quantum frustration makes the identification of these maximally entangled states particularly demanding and significant. In addition, the number of free parameters in quantum states and the number of bipartitions of the total system both grow exponentially with system size, making the investigation of multipartite entanglement and the search for MMES analytically and computationally very challenging [24, 28].

In this framework, *Hadamard states*, so named as they corresponds to a single row (or column) of a complex Hadamard matrix of the Butson class [31, 32], and characterized by equal weights in the computational basis, have been identified as compatible with MMES requirements, providing a structured class for theoretical and computational analysis [29]. Their intriguing properties, in terms of frustration and symmetries, make them promising candidates for investigating multipartite entanglement in qubit systems.

In this work, we characterize the entanglement properties of Hadamard states of n qubits using a statistical approach. We analyze different ensembles of Hadamard

states, having equal weights in the computational basis and phases independently and uniformly distributed over the q -th roots of unity, with $q = 2, 3, \dots$: *hypergraph states* ($q = 2$), introduced in Ref. [33], whose phases are the square roots of unity, either 1 or -1 and which correspond to a row (or column) of a real Hadamard matrix of the Butson class; the *Hadamard-Butson P_q -states* ($q = 3, 4, \dots$), whose possible phases are the vertices of a regular q -polygon, namely, $e^{i\frac{2\pi r}{q}}$, with $r = 0, \dots, q-1$; and *Hadamard-typical states* ($q = \infty$), whose phases are uniformly distributed over the unit circle. Notice that Hadamard-typical states are locally maximally entangleable states (LMES), as showed in Ref. [34].

Through analytical calculations and numerical simulations, we demonstrate that Hadamard ensembles exhibit, on average, a higher degree of entanglement than the Haar ensemble. Moreover, we show that the class of hypergraph states exhibits distinctive statistical properties that make them particularly promising for identifying MMES. In addition, hypergraph states occur naturally in the analysis of quantum algorithms such as the Deutsch-Jozsa algorithm and the Grover algorithm [33, 35] and, can be complex in the sense of Kolmogorov complexity, so they could, for instance, be used for quantum fingerprinting protocols [36]. Nonetheless, identifying MMES, even in the class of hypergraph states remains challenging, particularly as the system size increases.

The Article is structured as follows. In Sec. II, we introduce the necessary background and notation, review key results on Haar-typical states, and define the classes of Hadamard states under investigation. Section III is devoted to the evaluation of the first two cumulants of the purity distribution associated to a fixed bipartition, while Sec. IV extends the analysis to the purity averaged over all balanced bipartitions. Throughout, particular emphasis is placed on comparing the statistical entanglement features of Hadamard and Haar ensembles. Lastly, in Sec. V, we analyze the large-system limit of the purity distributions for Hadamard states and compare it with that of Haar-typical states.

II. PRELIMINARIES AND DEFINITIONS

We consider a system $S = \{1, \dots, n\}$ of n qubits, described by a Hilbert space of dimension $N = 2^n$,

$$\mathcal{H}_S = \bigotimes_{i \in S} \mathbb{C}_i^2 \simeq \mathbb{C}^N \quad (1)$$

A pure state of the system can be expressed in the computational basis as

$$|\psi\rangle = \sum_{k \in \mathbb{B}^n} z_k |k\rangle, \quad (2)$$

where $\mathbb{B} = \{0, 1\}$, $k = (k_1, \dots, k_n)$ with $k_i \in \mathbb{B}$, $|k\rangle = \bigotimes_{i \in S} |k_i\rangle_i$, $|k_i\rangle_i \in \mathbb{C}_i^2$, and the normalization condition $\sum_k |z_k|^2 = 1$ holds.

A bipartition of the system is defined by a pair (A, \bar{A}) , where $A \subset S$, $\bar{A} = S \setminus A$, and $1 \leq n_A \leq n_{\bar{A}}$, with $n_A = |A|$. A bipartition is said to be *balanced* if $n_A = \lfloor n/2 \rfloor$.

Given a bipartition (A, \bar{A}) and a pure state $|\psi\rangle$, the purity of subsystem A is defined as

$$\pi_A = \text{Tr}(\rho_A^2), \quad \rho_A = \text{Tr}_{\bar{A}}(|\psi\rangle\langle\psi|). \quad (3)$$

The purity quantifies the degree of entanglement between the two subsystems: lower values of π_A indicate stronger entanglement. For a subsystem of n_A qubits, the purity is bounded as

$$\frac{1}{2^{n_A}} \leq \pi_A \leq 1. \quad (4)$$

The purity of a fixed bipartition (A, \bar{A}) has the following expression [26]:

$$\pi_A(\mathbf{z}) = \sum_{k \in \mathbb{B}^n} \sum_{l \in \mathbb{B}^A} \sum_{m \in \mathbb{B}^{\bar{A}}} z_k z_{k \oplus l}^* z_{k \oplus l \oplus m} z_{k \oplus m}^*, \quad (5)$$

where \oplus is the bitwise XOR operation. This quantity describes the entanglement of the single bipartition (A, \bar{A}) , and fails in capturing the entanglement properties of the system as a whole.

A quantification of global multipartite entanglement for pure states is provided by the *potential of multipartite entanglement*, defined as the average purity over all balanced bipartitions [25],

$$\pi_{\text{ME}} = \binom{n}{\lfloor \frac{n}{2} \rfloor}^{-1} \sum_{|A|=\lfloor \frac{n}{2} \rfloor} \pi_A. \quad (6)$$

This quantity can be expressed as follows in terms of the state's Fourier coefficients $\mathbf{z} = (z_1, \dots, z_N)$ [25, 29]:

$$\pi_{\text{ME}}(\mathbf{z}) = \sum_{k, l, m \in \mathbb{B}^n} g(l, m) z_k z_{k \oplus l}^* z_{k \oplus l \oplus m} z_{k \oplus m}^*, \quad (7)$$

where

$$g(l, m) = \delta_{l \wedge m, 0} \hat{g}(|l|, |m|), \quad (8a)$$

$$\hat{g}(s, t) = \frac{1}{2} \binom{n}{\lfloor \frac{n}{2} \rfloor}^{-1} \left[\binom{n-s-t}{\lfloor \frac{n}{2} \rfloor - s} + \binom{n-s-t}{\lfloor \frac{n}{2} \rfloor - t} \right]. \quad (8b)$$

Here, $|l| = \sum_{i \in S} l_i$, while \wedge denotes the bitwise AND operation.

The average purity π_{ME} inherits the bounds (4) of the purity π_A of a fixed balanced bipartition, with $n_A = \lfloor n/2 \rfloor$, namely,

$$\frac{1}{2^{\lfloor \frac{n}{2} \rfloor}} \leq \pi_{\text{ME}} \leq 1. \quad (9)$$

Correspondingly, *maximally multipartite entangled states* (MMES) are defined as those minimizing the potential of multipartite entanglement (6).

In the case of a system of n qubits the minimal possible value of the potential of multipartite entanglement π_{ME} equals $2^{-\lfloor n/2 \rfloor}$. This theoretical bound for the minimum is saturated if perfect MMES or *Absolutely Maximally Entangled* (AME) states [37–41] exist. For $n = 2$ AME states are Bell states up to local unitary transformations, while for $n = 3$ they include the GHZ states [25, 38]. For $n = 5$ and $n = 6$, numerous examples of AME states have been identified [25]. Conversely, it has been proven that AME states do not exist for $n = 4$ [21], $n = 7$ [20, 22, 23], and $n \geq 8$ [20, 22], due to quantum frustration [24]. Frustration arises due to competing requirements among different bipartitions.

In the following we introduce Haar-typical and Hadamard states and review the main properties of the former.

A. Statistical Properties of Haar-Typical States

The unit sphere of states (2) of n qubits in \mathcal{H}_S ,

$$\mathbb{S}^{2N-1} = \left\{ \mathbf{z} = (z_1, \dots, z_N) \in \mathbb{C}^N : \sum_k |z_k|^2 = 1 \right\}, \quad (10)$$

is invariant under the action of the unitary group $U(\mathcal{H}_S) \simeq U(N)$, with $N = 2^n$, and Haar-typical pure states are sampled uniformly on \mathbb{S}^{2N} , according to the Haar measure of $U(N)$ [42].

The properties of Haar-typical pure states have been extensively studied [26, 27, 30, 42–47], and such states can be efficiently generated through chaotic dynamics [48]. The distribution of the purity referred to a fixed bipartition (A, \bar{A}) has mean and variance given by [26, 27, 44]

$$\mu_A = \langle \pi_A \rangle = \frac{2^{n_A} + 2^{n_{\bar{A}}}}{2^n + 1}, \quad (11)$$

$$\sigma_A^2 = \langle (\pi_A - \mu_A)^2 \rangle = \frac{2(2^{2n_A} - 1)(2^{2n_{\bar{A}}} - 1)}{(2^n + 1)^2(2^n + 2)(2^n + 3)}, \quad (12)$$

where $n_A = |A|$ is the number of qubits in subsystem A , $n_{\bar{A}} = n - n_A$, and $\langle \dots \rangle$ denotes the ensemble average over pure states uniformly distributed on \mathbb{S}^{2N-1} ,

$$\mathbf{z} \sim \text{Unif}(\mathbb{S}^{2N-1}). \quad (13)$$

The mean of π_{ME} is

$$\mu_{\text{ME}} = \langle \pi_{\text{ME}} \rangle = \mu_A, \quad (14)$$

with (A, \bar{A}) being any balanced bipartition, and thus it is given by (11) for $n_A = \lfloor n/2 \rfloor$,

$$\mu_{\text{ME}} = \frac{2^{\lfloor \frac{n}{2} \rfloor} + 2^{\lceil \frac{n}{2} \rceil}}{2^n + 1}. \quad (15)$$

The variance, $\sigma_{\text{ME}}^2 = \langle (\pi_{\text{ME}} - \mu_{\text{ME}})^2 \rangle$, is given by [30]

$$\sigma_{\text{ME}}^2 = \frac{(2^n + 1)f_2(n) - 2(2^{\lfloor \frac{n}{2} \rfloor} + 2^{\lceil \frac{n}{2} \rceil})^2}{(2^n + 1)^2(2^n + 2)(2^n + 3)}, \quad (16)$$

where

$$\begin{aligned} f_2(n) &= 4 \sum_{k,l \in \mathbb{B}^n} g(k,l)^2 \\ &= \sum_{s,t=0}^{\lfloor \frac{n}{2} \rfloor} \binom{n}{s,t}^{-1} \left[\binom{\lfloor \frac{n}{2} \rfloor}{s} \binom{\lceil \frac{n}{2} \rceil}{t} + \binom{\lfloor \frac{n}{2} \rfloor}{t} \binom{\lceil \frac{n}{2} \rceil}{s} \right]^2 \end{aligned} \quad (17)$$

with $\binom{n}{s,t} = \frac{n!}{s!t!(n-s-t)!}$ being the trinomial coefficient.

B. Hadamard States

For any pure state expressed in the computational basis, one can define the population probability vector $(P_S(k))_{k \in \mathbb{B}^n} = (|z_k|^2)_{k \in \mathbb{B}^n}$, whose components represent the probability of observing the computational basis state $|k\rangle$. The population probability vector of Haar-typical states (13) is uniformly distributed on the $(N-1)$ -dimensional probability simplex Δ_{N-1} , namely $P_S \sim \text{Uniform}(\Delta_{N-1})$ [49].

A necessary condition for a state to qualify as an AME state, and hence to saturate the theoretical minimum in (9), is that all the marginals over $n_A \leq n/2$ variables of its population probability vector, $P_S(k)$, are completely random [29].

A notable class of states satisfying this condition is the class of *Hadamard states*, defined by the property

$$|z_k|^2 = \frac{1}{2^n}, \quad \forall k \in \mathbb{B}^n, \quad (18)$$

which fixes the population probability vector at the center of the simplex Δ_{N-1} . Thus, for Hadamard states, the Fourier coefficients take the form,

$$z_k = \frac{s_k}{\sqrt{2^n}}, \quad s_k = e^{i\phi_k} \in \mathbb{S}, \quad \forall k \in \mathbb{B}^n, \quad (19)$$

with $\mathbb{S} = \{z \in \mathbb{C} : |z| = 1\}$ being the unit circle of complex numbers of unit modulus.

A central objective in the study of multipartite entanglement is the characterization of MMES, particularly in the context of frustrated systems, where AME states do not exist. However, MMES states are highly atypical and occur with vanishing probability under Haar measure [25]. In the case of n qubits, a generic pure state is described by $N = 2^n$ complex amplitudes $\mathbf{z} = (z_1, \dots, z_N)$, that correspond to a point on the $(2N-1)$ -dimensional sphere (10). This results in a high-dimensional optimization problem when attempting to minimize the average purity.

To address this challenge, it is useful to investigate classes of quantum states characterized by a reduced

Fourier coefficients $z_k = \frac{s_k}{\sqrt{2^n}}$	Notation
$s_k \in P_2 = \{+1, -1\}$	Hypergraph states ($q = 2$)
$s_k \in P_q = \left\{ e^{i\frac{2\pi r}{q}} \right\}_{r=0, \dots, q-1}$	Butson P_q -states ($q \geq 3$)
$s_k \in \mathbb{S} = \left\{ e^{i\phi} \right\}_{\phi \in [0, 2\pi]}$	Hadamard states ($q = \infty$)

TABLE I: Classification of Hadamard-Butson P_q -states ($q = 2, 3, \dots$) based on the possible values of the phases $s_k \in \mathbb{S}$ of their Fourier coefficients (19) in the computational basis.

number of parameters, while still satisfying the necessary condition for perfect MMES. It is known that Haar-typical states have Fourier coefficients with independently and uniformly distributed phases $s_k = z_k/|z_k| \sim \text{Unif}(\mathbb{S})$ [28, 49]. The approach adopted in this work retains this statistical feature while restricting the number of free parameters.

This motivates the study of the statistical properties of Hadamard states, particularly those whose phases s_k are in a finite number and symmetrically distributed on the unit circle \mathbb{S} . We refer to these as Hadamard-Butson P_q -states, for $q = 2, 3, \dots$, and they are listed in Table I. They are classified according to the allowed phases $s_k \in P_q$, taken to be the vertices of the regular polygon

$$P_q = \left\{ e^{i\frac{2\pi r}{q}} : r = 0, \dots, q-1 \right\} \quad (20)$$

of the q -th roots of unity. In particular, the Butson P_2 -states coincide with the hypergraph states, whose phases are restricted to ± 1 .

In the following analysis we will consider, as ensembles of random states, Hadamard-Butson P_q -states with phases independently and uniformly distributed over the polygon,

$$s_k \sim \text{Unif}(P_q), \quad k \in \mathbb{B}^n, \quad (21)$$

together with the limiting case $q = \infty$, corresponding to Hadamard-typical states, whose phases are independently and uniformly distributed over the entire unit circle,

$$s_k \sim \text{Unif}(\mathbb{S}), \quad k \in \mathbb{B}^n. \quad (22)$$

We will compare their statistical properties with those of the Haar-typical states discussed in the previous section.

III. FIRST TWO CUMULANTS OF THE PURITY AT FIXED BIPARTITION

In this section, we investigate the first two cumulants of the purity distribution associated with the classes of random Hadamard states listed in Table I.

As shown in Ref. [29], the purity corresponding to a fixed bipartition (A, \bar{A}) of a Hadamard state can be expressed as

$$\begin{aligned} \pi_A(\mathbf{s}) = & \frac{2^{n_A} + 2^{n_{\bar{A}}} - 1}{2^n} \\ & + \frac{1}{2^{2n}} \sum_{k \in \mathbb{B}^n} \sum_{l \in \mathbb{B}_{\bar{A}}^A} \sum_{m \in \mathbb{B}_{\bar{A}}^{\bar{A}}} s_k s_{k \oplus l}^* s_{k \oplus l \oplus m} s_{k \oplus m}^*, \end{aligned} \quad (23)$$

where $\mathbb{B}_*^m = \mathbb{B}^m \setminus \{0\}$ denotes the set of all nonzero m -bit binary strings. Importantly, since their indexes are all distinct, each term in the sum of Eq. (23) consists of four independent random variables of zero mean (21), and thus has zero average. Therefore, the mean of the purity distribution is given by the first term in (5), i.e.

$$\mu_A = \langle \pi_A \rangle = \frac{2^{n_A} + 2^{n_{\bar{A}}} - 1}{2^n}. \quad (24)$$

This allows us to write the purity as a sum of its average and a fluctuation term,

$$\pi_A(\mathbf{s}) = \mu_A + \tilde{\pi}_A(\mathbf{s}), \quad (25)$$

with $\tilde{\pi}_A$ being given by the second term in (23).

Consequently, the variance of the purity distribution is $\sigma_A^2 = \langle \tilde{\pi}_A^2 \rangle$ and is explicitly evaluated in Appendix A, yielding

$$\sigma_A^2 = 2c_q \frac{(2^{n_A} - 1)(2^{n_{\bar{A}}} - 1)}{2^{3n}}, \quad (26)$$

where

$$c_q = (1 + \delta_{q,2}), \quad (27)$$

for all Butson P_q -states (21) with $q \geq 2$, including Hadamard-typical states (22) ($q = \infty$).

Comparing the mean purities of Hadamard (24) and Haar ensembles (11), one finds that, for every bipartition (A, \bar{A}) ,

$$(\mu_A)_{\text{Hadamard}} < (\mu_A)_{\text{Haar}}. \quad (28)$$

Thus, Hadamard states exhibit, on average, a higher degree of entanglement than Haar states: imposing the condition (18) selects a subset of more entangled states.

Incidentally, observe that Eq. (24) generalizes to the full class of hypergraph states the results previously obtained in [50] via a tensor-network approach. In particular, it shows that the mean bipartite purity for hypergraph states coincides with that of graph states. Furthermore, Eq. (26) reveals that the fluctuations of bipartite entanglement across the ensemble of random hypergraph states exhibit the same scaling behavior identified in Ref. [50] for a specific subclass of this ensemble composed by purely hypergraph states, while scaling significantly faster than the fluctuations associated exclusively with graph states.

We benchmark the analytical results through extensive numerical simulations performed as described in Appendix B. The numerical data are shown in Figures 1a

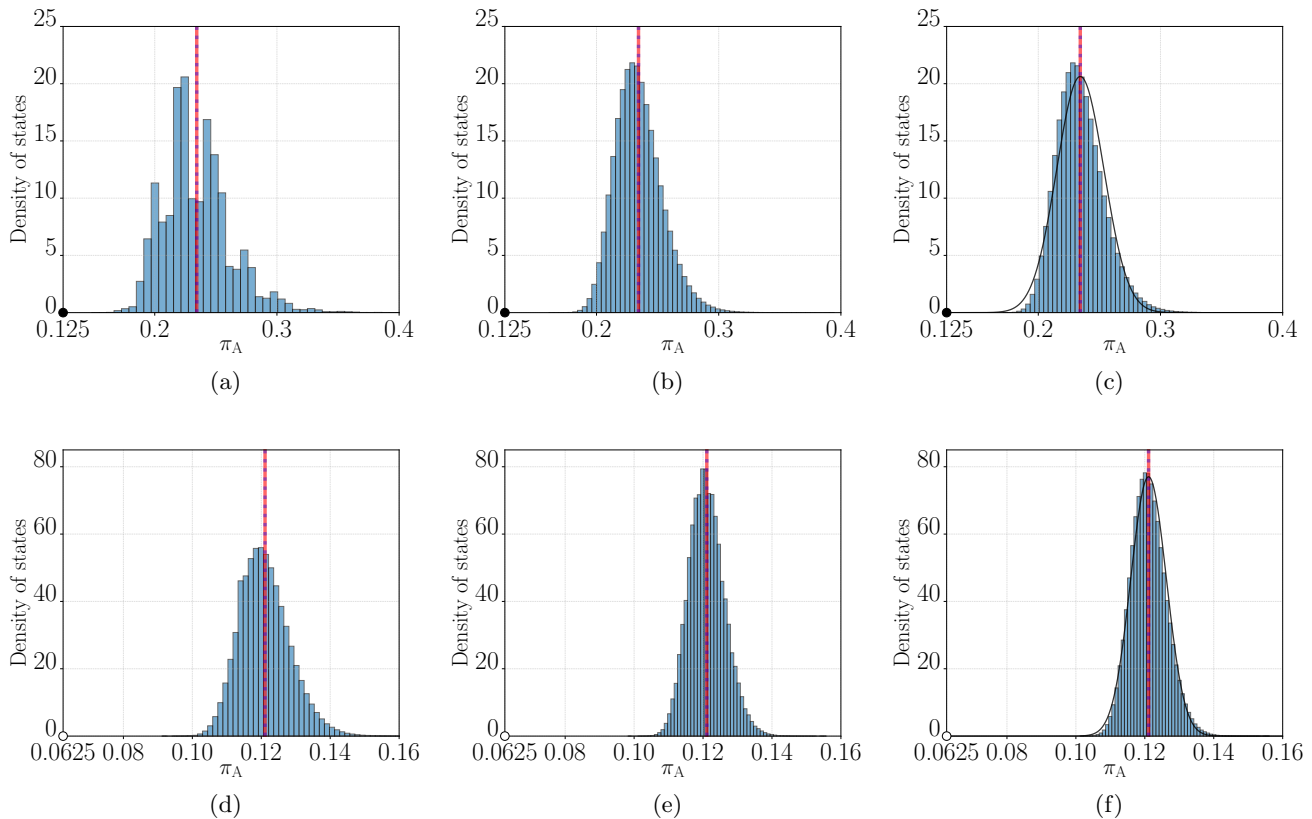


FIG. 1: Histograms of the purity distribution for the balanced bipartition (A, \bar{A}) with $A = \{1, \dots, \lfloor n/2 \rfloor\}$, based on 2.3×10^6 samplings of systems of $n = 6$ qubits (first row) and $n = 8$ qubits (second row) for Hadamard-Butson P_q -states: (a,d) hypergraph states ($q = 2$); (b,e) Butson P_4 -states and (c,f) Hadamard-typical states ($q = \infty$). In all the plots, the horizontal axis starts from the minimum value of π_A . Red lines indicate the theoretical value of the mean purity (24), while the (almost coinciding) dotted blue lines correspond to the numerically computed one. In c,f we have also plotted the Gaussians having mean and variance corresponding to the ones in Eqs. (24) and (26). We observe that the Gaussian approximation already provides an accurate description for $n = 8$. Notice that for $n = 6$ qubits, in the first line, there exist AME Hadamard states, with all purities of balanced bipartitions at the minimal value $1/8 = 0.125$, while for $n = 8$ qubits, in the second line, there exist no AME state, with all π_A having the minimal value $1/16 = 0.0625$, as highlighted by the full and empty dots on the horizontal axis, respectively.

and 1d for hypergraph states, in Figures 1b and 1e for Butson P_4 -states, and in Figures 1c and 1f for Hadamard-typical states. The results are in close agreement with the theoretical predictions given by Eqs. (24) and (26). Fig. 1 also highlights the discreteness of the purity spectra associated with the Butson P_q -states. However, as the qubit number increases, the purity distribution approximates a continuous one.

IV. FIRST TWO CUMULANTS OF THE AVERAGE PURITY

We now extend the previous analysis to the distribution of the average purity over all balanced bipartitions (6). Using the approach of Ref. [29], the average

purity for Hadamard P_q -states can be expressed as

$$\begin{aligned} \pi_{\text{ME}}(\mathbf{s}) &= \frac{2^{\lfloor \frac{n}{2} \rfloor} + 2^{\lceil \frac{n}{2} \rceil} - 1}{2^n} \\ &+ \frac{1}{2^{2n}} \sum_{k \in \mathbb{B}^n} \sum_{l, m \in \mathbb{B}_*^n} g(l, m) s_k s_{k \oplus l} s_{k \oplus l \oplus m} s_{k \oplus m}^*, \end{aligned} \quad (29)$$

where $g(l, m)$ is the coupling function (8a). From this expression, and proceeding analogously to that in Sec. III, we obtain

$$\mu_{\text{ME}} = \langle \pi_{\text{ME}} \rangle = \frac{2^{\lfloor \frac{n}{2} \rfloor} + 2^{\lceil \frac{n}{2} \rceil} - 1}{2^n}, \quad (30)$$

and

$$\pi_{\text{ME}}(\mathbf{s}) = \mu_{\text{ME}} + \tilde{\pi}_{\text{ME}}(\mathbf{s}), \quad (31)$$

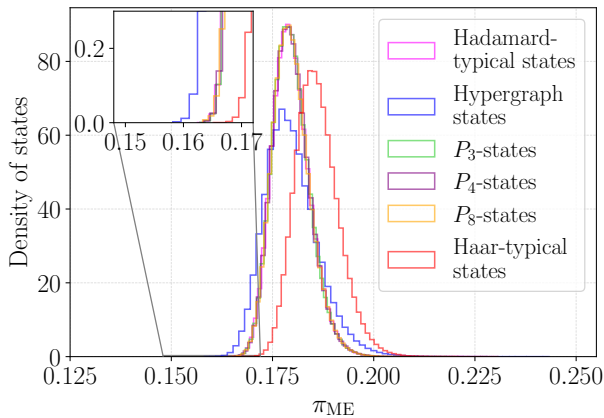


FIG. 2: Histograms of the average purity density for $n = 7$ qubits obtained from 2.3×10^6 samples of different ensembles of states. The horizontal axis starts from $\pi_{\text{ME}} = 1/8 = 0.125$, which corresponds to the theoretical bound for the minimum, which would be saturated, if seven-qubit AME states existed. Using Eq. (36), we observe that this value, is approximately 8.4 standard deviations from the mean value of the Hadamard-typical distribution.

where $\tilde{\pi}_{\text{ME}}(\mathbf{s})$ denotes the second term in Eq. (29).

By comparing (15) and (30), we get that

$$(\mu_{\text{ME}})_{\text{Hadamard}} < (\mu_{\text{ME}})_{\text{Haar}}, \quad (32)$$

which confirms that Hadamard states exhibit, on average, a higher degree of entanglement than Haar-distributed states.

It follows from (29) that the variance of the average purity distribution is given by $\sigma_{\text{ME}}^2 = \langle \tilde{\pi}_{\text{ME}}^2 \rangle$. This quantity is explicitly evaluated in Appendix A, yielding

$$\sigma_{\text{ME}}^2 = \frac{c_q}{2^{3n}} f_{2*}(n), \quad (33)$$

where $c_q = (1 + \delta_{q,2})$, for $q = 2, 3, \dots$, and

$$\begin{aligned} f_{2*}(n) &= 4 \sum_{k,l \in \mathbb{B}_n} g(k,l)^2 \\ &= \sum_{s,t=1}^{\lceil \frac{n}{2} \rceil} \binom{n}{s,t}^{-1} \left[\binom{\lfloor \frac{n}{2} \rfloor}{s} \binom{\lceil \frac{n}{2} \rceil}{t} + \binom{\lfloor \frac{n}{2} \rfloor}{t} \binom{\lceil \frac{n}{2} \rceil}{s} \right]^2. \end{aligned} \quad (34)$$

Since $f_{2*}(n) < f_2(n)$, one also gets

$$(\sigma_{\text{ME}})_{\text{Hadamard}} < (\sigma_{\text{ME}})_{\text{Haar}}, \quad (35)$$

for all $n \geq 4$ and all P_q -states with $q \neq 2$. Interestingly, the inequality is reversed for hypergraph states, $q = 2$.

In Fig. 2, we compare the distributions of the average purity across different classes of seven-qubit states

obtained through numerical simulations (details in Appendix B). The P_q -states exhibit statistical behavior similar to Hadamard-typical states up to the second cumulant. In contrast, hypergraph states ($q = 2$) display significantly broader distributions, as predicted by Eq. (33). All considered Hadamard states exhibit, on average, a higher degree of entanglement than Haar-typical pure states, consistently with Eq. (30) and Eq. (15).

The broader distribution of hypergraph states increases the probability of sampling low average purity states, making them promising candidates in the search for MMES, as highlighted by the inset of Fig. 2. Nevertheless, finding such states remains a formidable challenge, as indicated by the location of the theoretical bound for the minimum of the average purity (from which the horizontal axis in Fig. 2 starts). Specifically, we observe that, since

$$k = \frac{\mu_{\text{ME}} - 2^{-\lfloor \frac{n}{2} \rfloor}}{\sigma_{\text{ME}}} = \frac{(2^{\lfloor \frac{n}{2} \rfloor} - 1)2^{\frac{n}{2}}}{(c_q f_{2*}(n))^{\frac{1}{2}}}, \quad (36)$$

the theoretical minima, even in the case of hypergraph states, lie k standard deviations below the average value, with $k \simeq 2.9, 3.2, 7.5, 8.4$, and 19 for $n = 4, 5, 6, 7$, and 8, respectively.

We further extend our analysis to different system sizes by numerically simulating systems up to 12 qubits. In Fig. 3, we show analytical (solid lines) and numerical (scattered points) values of the mean and standard deviation of the average purity distribution for all classes of states. Analytical results are given by: Eq. (15) and the square root of Eq. (16) for Haar-typical ensembles; Eq. (30) and the square root of Eq. (33) for all Hadamard ensembles. All the numerical results are in strong agreement with the analytical predictions, confirming the distinctive properties of hypergraph states (P_2 -states).

V. LARGE-SYSTEM LIMIT

As shown in Sec. III, the fluctuating part $\tilde{\pi}_A(\mathbf{s})$ of the purity of a fixed bipartition of a Hadamard state (23) consists of $O(2^{2n})$ terms of order $O(1/2^{2n})$. For a large number n of qubits, the purity distribution of Hadamard states referred to a fixed bipartition is close to a Gaussian distribution with mean given by Eq. (24) and variance given by Eq. (26).

The asymptotic mean of the purity distributions of Hadamard states (24) coincides with that of Haar-typical states (11),

$$\mu_A \sim \frac{1}{2^{n_A}} + \frac{1}{2^{n_{\bar{A}}}}, \quad (37)$$

as $n \rightarrow \infty$. This occurs because the fluctuations in the moduli of the components a unit random vector become relatively small as the vector length increases, so a generic random vector effectively behaves like one with equal moduli.

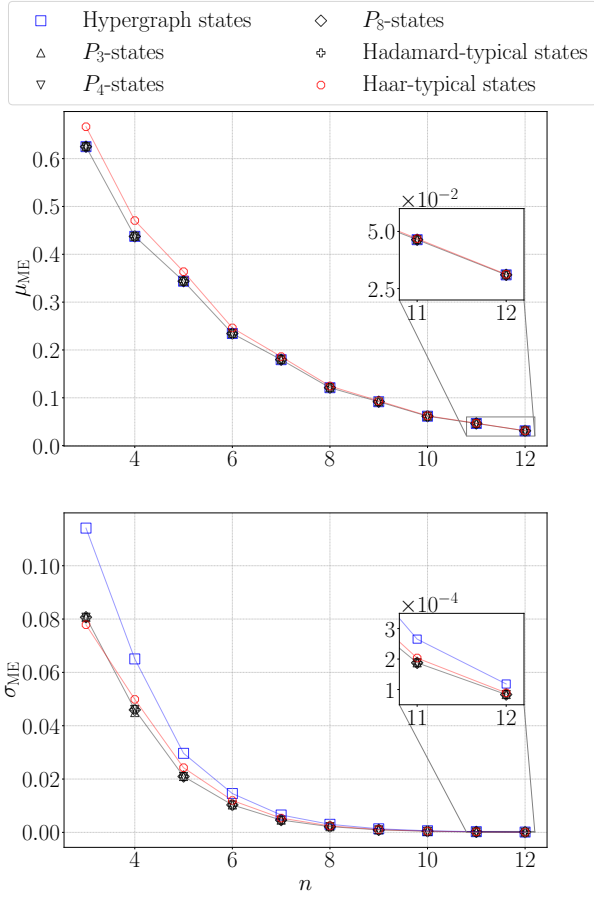


FIG. 3: Mean and standard deviation of the average purity distribution as a function of system size, showing theoretical predictions (solid lines) and numerical results (scattered points) for Haar-typical states (red), hypergraph states (blue), Butson P_3 -, P_4 -, P_8 -states and Hadamard-typical states (black).

Similarly, the asymptotic behavior of the variance (26) of the purity distribution for the Hadamard ensembles is

$$\sigma_A^2 \sim c_q \frac{2}{2^{2n}}, \quad (38)$$

as $n \rightarrow \infty$, where $c_q = 1 + \delta_{q,2}$. Thus, it is asymptotically equivalent to the variance (12) of the Haar ensemble, except in the special case $q = 2$, corresponding to hypergraph states, where it is twice as large.

For large n , the distribution of the average purity π_{ME} of Haar-typical states is also approximately Gaussian [28]. Its mean (15) behaves as

$$\mu_{\text{ME}} \sim \frac{1}{2^{\frac{n}{2}}} \begin{cases} 2 & \text{if } n \text{ even} \\ \frac{3}{\sqrt{2}} & \text{if } n \text{ odd} \end{cases}, \quad (39)$$

as $n \rightarrow \infty$. Moreover, the function in (17) has the fol-

lowing asymptotics [30]:

$$f_2(n) \sim 3\sqrt{2} \left(\frac{3}{2}\right)^n = 3\sqrt{2} 2^{\alpha n}, \quad (40)$$

as $n \rightarrow \infty$, where

$$\alpha = \log_2 \left(\frac{3}{2}\right) \simeq 0.58. \quad (41)$$

Therefore, the variance σ_{ME}^2 given by (16), behaves as

$$\sigma_{\text{ME}}^2 \sim 3\sqrt{2} \left(\frac{3}{16}\right)^n = 3\sqrt{2} \frac{1}{2^{(3-\alpha)n}}. \quad (42)$$

Analogous considerations apply to the average purity of ensembles of Hadamard states, expressed by Eq. (29), which also consists of at most 2^{2n} terms of order $O(1/2^{2n})$, and for large n is close to a Gaussian with mean being given by Eq. (30), and variance being provided by Eq. (33) for all the ensembles of Hadamard P_q -states.

For large n , the mean (30) of the Hadamard ensembles has the same asymptotics (14) of the Haar ensemble. Moreover, as derived in Appendix C, the function f_{2*} has the same asymptotic behavior (17) of f_2 , namely,

$$f_{2*}(n) \sim 3\sqrt{2} \left(\frac{3}{2}\right)^n = 3\sqrt{2} 2^{\alpha n}, \quad (43)$$

as $n \rightarrow \infty$. Therefore, in this limit, the variance of the average purity distribution becomes

$$\sigma_{\text{ME}}^2 \sim 3\sqrt{2} c_q \left(\frac{3}{16}\right)^n = 3\sqrt{2} c_q \frac{1}{2^{(3-\alpha)n}}, \quad (44)$$

with $c_q = (1 + \delta_{q,2})$, for all ensembles of Hadamard states in Table I.

Thus, in the large-system limit, all Hadamard states, except the hypergraph states, exhibit the same asymptotic purity distribution as Haar states.

However, notice that Hadamard states retain an entanglement advantage: the distance between the averages scales as

$$\Delta\mu_{\text{ME}} = (\mu_{\text{ME}})_{\text{Haar}} - (\mu_{\text{ME}})_{\text{Hadamard}} \sim \frac{1}{2^n}, \quad (45)$$

while the variances scale as in Eqs. (42) and (44), that is $\sigma_{\text{ME}} = O((3/16)^{n/2})$. Thus,

$$\frac{\sigma_{\text{ME}}}{\Delta\mu_{\text{ME}}} = O\left(\left(\frac{3}{8}\right)^{\frac{n}{2}}\right) \quad (46)$$

and the distributions of Hadamard states and Haar-typical states remain statistically distinct even for large systems. Furthermore, the hypergraph states retain a particular feature in the high-entanglement regime, showing increased probabilities even in the large-system limit. This distinctive scaling behavior, also highlighted by the inset of Fig. 3, makes hypergraph states uniquely valuable for exploring extreme entanglement even in large qubit systems.

VI. CONCLUDING REMARKS AND OUTLOOK

We systematically investigated the statistical properties of the purity and average purity for various ensembles of Hadamard states of qubits. By extending the approach pioneered in Refs. [28, 30, 47], we derived exact analytical expressions for the first and second cumulants of these distributions. We also performed extensive numerical simulations to validate these analytical results. We showed that all considered Hadamard states exhibit on average a higher degree of entanglement than typical (Haar-distributed) states.

Our analysis also revealed the unique properties of hypergraph states, whose purity fluctuations are significantly larger than those of the other ensembles of Hadamard P_q -states. The increased variance in the purity distribution of the hypergraph states suggests a higher probability of sampling states that approach the theoretical minimum of the average purity, even for large systems. This makes the hypergraph states promising candidates in the ongoing search for MMES.

An interesting future direction would be the extension of our cumulant analysis to higher-order moments, which could deepen the statistical characterization of purity distribution and potentially unveil additional features of Hadamard states compared to typical ones. Moreover, while MMES have been extensively studied among typical states [24], an extensive numerical and analytical analysis of MMES among Hadamard states, and particularly among hypergraph states, is still missing.

The identification and characterization of highly entangled multipartite states have implications beyond fundamental physics. Such states are crucial resources for quantum algorithms, particularly in quantum optimization protocols and certain quantum machine learning schemes where entanglement enables the efficient exploration of large solution spaces [51–57]. Additionally, understanding multipartite entanglement is relevant for developing and analyzing quantum error correcting codes [22, 58, 59].

In summary, this work deepens our understanding of multipartite entanglement through statistical lens, revealing distinctive properties of Hadamard quantum states that suggest promising directions for future research.

VII. ACKNOWLEDGMENTS

We thank Chiara Macchiavello and Flavio Baccari for useful discussions and feedback on our work.

We acknowledge support from INFN through the project “QUANTUM” and from the Italian funding within the “Budget MUR - Dipartimenti di Eccellenza 2023–2027” - Quantum Sensing and Modelling for One-Health (QuaSiModO). PF acknowledges support from the Italian National Group of Mathematical Physics (GNFM-INdAM) and from PNRR MUR project

CN00000013-“Italian National Centre on HPC, Big Data and Quantum Computing“. GM acknowledges support from the University of Bari via the 2023-UNBACLE-0244025 grant and from INFN through the project “NPQCD”. SP acknowledges support from PNRR MUR project PE0000023-NQSTI. KŽ acknowledges funding by the European Union under ERC 722 Advanced Grant TAtypic, Project No. 101142236. We acknowledge computational resources provided by the University of Bari and the INFN cluster ReCaS [60].

Appendix A: Computation of the variances

As shown in Sec. III, the variance of the purity distribution associated with Hadamard states and referred to a fixed bipartition is $\sigma_A^2 = \langle \tilde{\pi}_A^2 \rangle$, where $\tilde{\pi}_A$ is given in the second line of (23). Explicitly,

$$\sigma_A^2 = \frac{1}{2^{4n}} \left\langle \left(\sum_{k \in \mathbb{B}^n} \sum_{l \in \mathbb{B}_*^A} \sum_{m \in \mathbb{B}_*^{\bar{A}}} s_k s_{k \oplus l}^* s_{k \oplus l \oplus m} s_{k \oplus m}^* \right) \times \left(\sum_{p \in \mathbb{B}^n} \sum_{v \in \mathbb{B}_*^A} \sum_{r \in \mathbb{B}_*^{\bar{A}}} s_p s_{p \oplus v}^* s_{p \oplus v \oplus r} s_{p \oplus r}^* \right) \right\rangle, \quad (\text{A1})$$

that is

$$\sigma_A^2 = \frac{1}{2^{4n}} \sum_{k, p \in \mathbb{B}^n} \sum_{l, v \in \mathbb{B}_*^A} \sum_{m, r \in \mathbb{B}_*^{\bar{A}}} \langle (s_k s_{k \oplus l}^* s_{k \oplus l \oplus m} s_{k \oplus m}^*) (s_p s_{p \oplus v}^* s_{p \oplus v \oplus r} s_{p \oplus r}^*) \rangle. \quad (\text{A2})$$

For the Hadamard ensembles considered here, the variables s_k are independent random phases, uniformly distributed on the regular polygon P_q , and $|s_k|^2 = 1$. Hence, the expectation value of any product of such phases is non-zero only if, for each index $k \in \mathbb{B}^n$, the number of occurrences of s_k equals the number of occurrences of s_k^* . Equivalently, the set of four indices carried by the unconjugated phase factors must coincide with the set of four indices carried by the conjugated phase factors.

In the present case, since l, m (and v, r) are non-zero and have support on complementary subsystems, no cancellation can occur within a single 4-phase factor. Therefore, the only non-vanishing contributions arise when the indices of the unconjugated phases in one factor are paired with the indices of the conjugated phases in the other one, and vice versa. This can happen in two ways, namely when $k = p \oplus v$ or when $k = p \oplus r$, which then fixes the remaining indices.

Let us illustrate this with the case $k = p \oplus v$. Then one unconjugated phase factor from the first parenthesis in (A2) is paired with one conjugated phase factor from the second parenthesis. For the remaining phase factors to give a non-zero expectation value, their indices must also match, which imposes $l \oplus m = v \oplus r$. The remaining product is therefore $s_{k \oplus l}^* s_{k \oplus m}^* s_{k \oplus v} s_{k \oplus v \oplus l \oplus m}$.

A non-vanishing contribution is obtained only when either $l = v$ or $m = v$. However, since $v \in \mathbb{B}_*^A$, whereas $m \in \mathbb{B}_*^{\bar{A}}$, the latter possibility is excluded. Thus the only admissible solution in this case is $l = v$, and consequently $m = r$. The case $k = p \oplus r$ is analogous.

Accordingly, the variance reads

$$\begin{aligned} \sigma_A^2 &= \frac{1}{2^{4n}} \sum_{k,p \in \mathbb{B}^n} \sum_{l,v \in \mathbb{B}_*^A} \sum_{m,r \in \mathbb{B}_*^{\bar{A}}} (\delta_{k,p \oplus v} + \delta_{k,p \oplus r}) \delta_{l,v} \delta_{m,r} \\ &= \frac{1}{2^{4n}} \sum_{p \in \mathbb{B}^n} \sum_{v \in \mathbb{B}_*^A} \sum_{r \in \mathbb{B}_*^{\bar{A}}} 2 = 2 \frac{(2^{n_A} - 1)(2^{n_{\bar{A}}} - 1)}{2^{3n}}. \end{aligned} \quad (\text{A3})$$

For hypergraph states ($q = 2$), whose coefficients are real, one has $s_k^2 = s_k^{*2} = 1$. As a result, additional non-zero contributions arise from direct pairings of the phases s across the two parentheses. This happens when $k = p$ or $k = p \oplus v \oplus r$ which, similarly to the previously discussed cases, fix all other indices. Together with the conditions originating from the pairing between phase factors s and conjugated phase factors s^* , these yield four distinct matching configurations, leading to the contribution

$$(\delta_{k,p \oplus v} + \delta_{k,p \oplus r} + \delta_{k,p} + \delta_{k,p \oplus v \oplus r}) \delta_{l,v} \delta_{m,r}. \quad (\text{A4})$$

This effectively doubles the number of contributing configurations with respect to the other Hadamard ensembles.

As a result, the variance of the purity distribution for Hadamard P_q -states and referred to a fixed bipartition is given by

$$\sigma_A^2 = 2c_q \frac{(2^{n_A} - 1)(2^{n_{\bar{A}}} - 1)}{2^{3n}}, \quad (\text{A5})$$

with

$$c_q = (1 + \delta_{q,2}), \quad (\text{A6})$$

for all $q \geq 2$, including Hadamard-typical states ($q = \infty$).

A similar analysis applies to the computation of the variance of the average purity distribution. As showed in Sec. IV, this quantity is given by $\sigma_{\text{ME}}^2 = \langle (\tilde{\pi}_{\text{ME}})^2 \rangle$, which explicitly reads

$$\begin{aligned} \sigma_{\text{ME}}^2 &= \frac{1}{2^{4n}} \sum_{k,p \in \mathbb{B}^n} \sum_{l,m,v,r \in \mathbb{B}_*^n} g(l,m) g(q,r) \\ &\quad \times \langle s_k s_{k \oplus l}^* s_{k \oplus l \oplus m} s_{k \oplus m}^* s_p s_{p \oplus v}^* s_{p \oplus v \oplus r} s_{p \oplus r}^* \rangle. \end{aligned} \quad (\text{A7})$$

As in the fixed bipartition case, the non-vanishing contributions to the variance arise from matching index configurations between the s -terms and their conjugates. However, in this case, the conditions $k = p \oplus v$ or $k = p \oplus r$ do not fully fix the remaining indices. For instance, if $k = p \oplus v$, then the relevant term becomes $s_{k \oplus l}^* s_{k \oplus m}^* s_{k \oplus v} s_{k \oplus v \oplus l \oplus m}$, which contributes non-trivially

when either $l = v$ or $m = v$. Since $l, m, v, r \in \mathbb{B}_*^n$, both configurations are admissible, resulting in four valid matchings for all P_q -states with $q \geq 3$. In contrast, for $q = 2$, non-vanishing contributions also arise from configurations in which the s -terms of both factors are directly matched. This leads to eight distinct non-vanishing terms, thereby doubling the number of contributing terms compared to the other ensembles.

Summarizing the above, we find that

$$\sigma_{\text{ME}}^2 = \frac{4c_q}{2^{3n}} \sum_{l,m \in \mathbb{B}_*^n} g(l,m)^2, \quad (\text{A8})$$

with $c_q = (1 + \delta_{q,2})$. We get

$$\begin{aligned} f_{2^*}(n) &= 4 \sum_{k,l \in \mathbb{B}_*^n} g(k,l)^2 = 4 \sum_{k,l \in \mathbb{B}_*^n} \delta_{k \wedge l, 0} \hat{g}(|k|, |l|)^2 \\ &= \sum_{1 \leq s, t \leq n} 4 \hat{g}(s,t)^2 \sum_{k,l \in \mathbb{B}_*^n} \delta_{k \wedge l, 0} \delta_{|k|,s} \delta_{|l|,t} \\ &= \sum_{1 \leq s, t \leq n} 4 \hat{g}(s,t)^2 \binom{n}{s,t} \\ &= \sum_{s,t=1}^{\lfloor \frac{n}{2} \rfloor} \binom{n}{s,t}^{-1} \left[\binom{\lfloor \frac{n}{2} \rfloor}{s} \binom{\lfloor \frac{n}{2} \rfloor}{t} + \binom{\lfloor \frac{n}{2} \rfloor}{t} \binom{\lfloor \frac{n}{2} \rfloor}{s} \right]^2, \end{aligned} \quad (\text{A9})$$

where we used the straightforward identity

$$\begin{aligned} \hat{g}(s,t) &= \frac{1}{2} \binom{n}{\lfloor \frac{n}{2} \rfloor}^{-1} \left[\binom{n-s-t}{\lfloor \frac{n}{2} \rfloor - s} + \binom{n-s-t}{\lfloor \frac{n}{2} \rfloor - t} \right] \\ &= \frac{1}{2} \binom{n}{s,t}^{-1} \left[\binom{\lfloor \frac{n}{2} \rfloor}{s} \binom{\lfloor \frac{n}{2} \rfloor}{t} + \binom{\lfloor \frac{n}{2} \rfloor}{t} \binom{\lfloor \frac{n}{2} \rfloor}{s} \right] \end{aligned} \quad (\text{A10})$$

on the function $\hat{g}(s,t)$ defined in (8b). By plugging (A9) into (A8) we obtain the result (33)–(34) of the main text.

Appendix B: Numerical simulations

A Haar-typical pure quantum state of n -qubits can be obtained by acting with a random unitary operator, sampled according to the Haar measure, on a generic reference state. In other words, a typical state corresponds to a single row (or column) of a unitary matrix sampled according to the Haar measure [42]. Based on this observation, we simulated typical states by generating full unitary matrices sampled from the Haar distribution using the algorithm presented in [61].

Hadamard states, in contrast, are characterized by a reduced number of parameters compared to Haar states, which makes their numerical simulation significantly simpler.

To simulate a Hadamard pure state of an n -qubits system, we constructed an ordered list of $N = 2^n$ phases

($s_k = e^{i\phi_k}$), uniformly sampled from the regular polygon defining the chosen class of Hadamard states, as reported in Table I. The vector of Fourier coefficient (z_1, \dots, z_N) was then obtained using Eq. (19). This procedure is computationally less demanding than generating a random unitary matrix. We performed simulations for P_2, P_3, P_4, P_8 -states and Hadamard-typical states.

For all mentioned ensembles of Hadamard states, as well as for the Haar ensemble, we generated $2.3 \cdot 10^6$ states for system sizes ranging from $n = 3$ to $n = 12$ qubits. In addition, due to the reduced dimension of the states space, we were able to generate all possible hypergraph states with $n = 3, 4$ and P_3 - and P_4 -states with $n = 3$.

For both Hadamard and Haar states, we first computed the purity referred to the bipartition $A = \{1, \dots, \lfloor n/2 \rfloor\}$. Then, we generated the list of all the possible balanced bipartitions, computed the purity for each case and evaluated the average purity as their arithmetic mean. Although the simulations of the purity referred to a fixed bipartition are specific to $A = \{1, \dots, \lfloor n/2 \rfloor\}$, the results are independent of this choice as the purity distributions are statistically independent of the specific bipartition [26].

All numerical simulations were performed on the RE-CAS computing cluster [60], utilizing up to 64 cores and 32 GB of memory per job.

Appendix C: Asymptotic behavior of $f_{2*}(n)$

The summation in the expression (34) of f_{2*} can be split as

$$4 \left(\sum_{l, m \in \mathbb{B}^n} g(l, m)^2 - 2 \sum_{l \in \mathbb{B}^n} g(l, 0)^2 + 1 \right), \quad (\text{C1})$$

where we have used the fact that $g(0, 0) = 1$. Therefore, we have

$$f_{2*}(n) = f_2(n) - 2h_2(n) + 4, \quad (\text{C2})$$

where $f_2(n)$ is defined in Eq. (17) and

$$h_2(n) = 4 \sum_{l \in \mathbb{B}^n} g(l, 0)^2. \quad (\text{C3})$$

This is the contribution with $t = 0$ of the sum in the second line of (17), namely,

$$h_2(n) = \sum_{s=0}^{\lfloor \frac{n}{2} \rfloor} \binom{n}{s}^{-1} \left[\binom{\lfloor \frac{n}{2} \rfloor}{s} + \binom{\lceil \frac{n}{2} \rceil}{s} \right]^2. \quad (\text{C4})$$

We derive the asymptotic behavior of the function $h_2(n)$ defined in Eq. (C4). Let us consider the case of even n :

$$h_2(n) = 4 \sum_{0 \leq s \leq \frac{n}{2}} \binom{n}{s}^{-1} \binom{\frac{n}{2}}{s}^2. \quad (\text{C5})$$

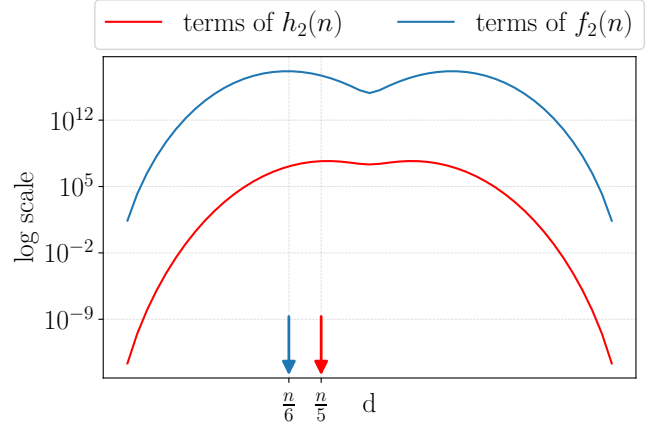


FIG. 4: Comparison between the terms appearing in the sums defining $f_2(n)$ in (C13) and $h_2(n)$ in (C14) versus the distance d (C12) between pairs of bipartitions, in logarithmic scale. We set $n = 100$. The maxima of the terms of both sums, expressed as fractions of n , are highlighted.

This summation depends on the ratio s/n , which we can define as a new variable

$$x = \frac{s}{n}. \quad (\text{C6})$$

By Stirling approximation $n! \sim (n/e)^n \sqrt{2\pi n}$ we obtain

$$\begin{aligned} h_2(n) &\sim \frac{4}{\sqrt{2\pi n}} \sum_{0 \leq s \leq \frac{n}{2}} \sqrt{\frac{1-x}{x}} \frac{1}{1-2x} e^{n[H(2x)-H(x)]} \\ &\sim 4 \sqrt{\frac{n}{2\pi}} \int_0^{\frac{1}{2}} dx \sqrt{\frac{1-x}{x}} \frac{1}{1-2x} e^{n[H(2x)-H(x)]}, \end{aligned} \quad (\text{C7})$$

where

$$H(x) = -x \ln x - (1-x) \ln(1-x) \quad (\text{C8})$$

is the Shannon entropy of x . It is easy to see that the exponent $H(2x) - H(x)$ takes its maximum at $x_0 = (2 - \sqrt{2})/4$, and using the saddle point approximation we get

$$\begin{aligned} h_2(n) &\sim 4 \sqrt{\frac{n}{2\pi}} \sqrt{\frac{1-x_0}{x_0}} \frac{1}{1-2x_0} e^{n[H(2x_0)-H(x_0)]} \\ &\quad \times \int_0^{1/2} dx e^{\frac{n}{2}[4H''(2x_0)-H''(x_0)](x-x_0)^2} \\ &\sim 4 \sqrt{\frac{n}{2\pi}} (2 + \sqrt{2}) e^{n \log\left(\frac{1+\sqrt{2}}{2}\right)} \int_{\mathbb{R}} dx e^{-4\sqrt{2}nx^2} \\ &= 2^{1/4} (2 + \sqrt{2}) \left(\frac{1 + \sqrt{2}}{2}\right)^n \\ &= 2^{1/4} (2 + \sqrt{2}) 2^{\gamma n}, \end{aligned} \quad (\text{C9})$$

where

$$\gamma = \log_2 \left(\frac{1 + \sqrt{2}}{2} \right) \simeq 0.27. \quad (\text{C10})$$

For odd n , the asymptotic expression (C9) acquires the additional factor $(4 + 3\sqrt{2})/8$.

Therefore, the function $h_2(n)$ is asymptotically negligible with respect to the asymptotic behavior (40) of $f_2(n)$, since $\alpha > 2\gamma$. It follows that, for large n , $f_{2*}(n)$ is asymptotically equivalent to $f_2(n)$, namely,

$$f_{2*}(n) \sim 3\sqrt{2} \left(\frac{3}{2}\right)^n = 3\sqrt{2} 2^{\alpha n}, \quad (\text{C11})$$

as $n \rightarrow \infty$.

In Ref. [30], it was shown that the sum (17) defining $f_2(n)$ can be expressed in terms of the distance

$$d = |A \cap \bar{B}| \quad (\text{C12})$$

between two bipartitions (A, \bar{A}) and (B, \bar{B}) , as

$$f_2(n) = \binom{n}{\lfloor \frac{n}{2} \rfloor}^{-1} \sum_{d=0}^{\lfloor \frac{n}{2} \rfloor} \binom{\lfloor \frac{n}{2} \rfloor}{d} \binom{\lceil \frac{n}{2} \rceil}{d} 2^{\frac{n}{2}+1} \times \left[2^{\frac{n}{2}-2d} + 2^{-(\frac{n}{2}-2d)} \right]. \quad (\text{C13})$$

The corresponding expression for $h_2(n)$ reads

$$h_2(n) = \binom{n}{\lfloor \frac{n}{2} \rfloor}^{-1} \sum_{d=0}^{\lfloor \frac{n}{2} \rfloor} \binom{\lfloor \frac{n}{2} \rfloor}{d} \binom{\lceil \frac{n}{2} \rceil}{d} \times \left[(2^{\lfloor \frac{n}{2} \rfloor} + 2^{\lceil \frac{n}{2} \rceil}) 2^{-d} + 2^{d+1} \right]. \quad (\text{C14})$$

The comparison between the terms in the sums (C13) and (C14) is shown in Fig. 4 in the deep asymptotic regime, at $n = 100$, confirming the asymptotic dominance of f_2 over h_2 .

-
- [1] C. H. Bennett, G. Brassard, C. Crépeau, R. Jozsa, A. Peres, and W. K. Wootters, Teleporting an unknown quantum state via dual classical and Einstein-Podolsky-Rosen channels, *Phys. Rev. Lett.* **70**, 1895 (1993).
- [2] D. Bouwmeester, J.-W. Pan, K. Mattle, M. Eibl, H. Weinfurter, and A. Zeilinger, Experimental quantum teleportation, *Nature* **390**, 575–579 (1997).
- [3] D. Boschi, S. Branca, F. De Martini, L. Hardy, and S. Popescu, Experimental realization of teleporting an unknown pure quantum state via dual classical and Einstein-Podolsky-Rosen channels, *Phys. Rev. Lett.* **80**, 1121 (1998).
- [4] M. A. Nielsen and I. L. Chuang, *Quantum Computation and Quantum Information* (Cambridge University Press, 2000).
- [5] G. Alber, T. Beth, M. Horodecki, P. Horodecki, R. Horodecki, M. Rötteler, H. Weinfurter, R. Werner, and A. Zeilinger, *Quantum Information: An Introduction to Basic Theoretical Concepts and Experiments* (Springer, 2001).
- [6] C. H. Bennett and G. Brassard, Quantum cryptography: Public key distribution and coin tossing, *Theoretical Computer Science* **560**, 7 (2014), theoretical Aspects of Quantum Cryptography – celebrating 30 years of BB84.
- [7] A. K. Ekert, Quantum cryptography based on Bell’s theorem, *Phys. Rev. Lett.* **67**, 661 (1991).
- [8] D. Deutsch, A. Ekert, R. Jozsa, C. Macchiavello, S. Popescu, and A. Sanpera, Quantum privacy amplification and the security of quantum cryptography over noisy channels, *Phys. Rev. Lett.* **77**, 2818 (1996).
- [9] C. A. Fuchs, N. Gisin, R. B. Griffiths, C.-S. Niu, and A. Peres, Optimal eavesdropping in quantum cryptography. i. information bound and optimal strategy, *Phys. Rev. A* **56**, 1163 (1997).
- [10] C. H. Bennett, D. P. DiVincenzo, J. A. Smolin, and W. K. Wootters, Mixed-state entanglement and quantum error correction, *Phys. Rev. A* **54**, 3824 (1996).
- [11] W. K. Wootters, Entanglement of formation of an arbitrary state of two qubits, *Phys. Rev. Lett.* **80**, 2245 (1998).
- [12] W. K. Wootters, Entanglement of formation and concurrence, *Quantum Info. Comput.* **1**, 27–44 (2001).
- [13] D. Bruß, Characterizing entanglement, *Journal of Mathematical Physics* **43**, 4237 (2002).
- [14] L. Amico, R. Fazio, A. Osterloh, and V. Vedral, Entanglement in many-body systems, *Rev. Mod. Phys.* **80**, 517 (2008).
- [15] R. Horodecki, P. Horodecki, M. Horodecki, and K. Horodecki, Quantum entanglement, *Rev. Mod. Phys.* **81**, 865 (2009).
- [16] V. Coffman, J. Kundu, and W. K. Wootters, Distributed entanglement, *Phys. Rev. A* **61**, 052306 (2000).
- [17] A. Wong and N. Christensen, Potential multiparticle entanglement measure, *Phys. Rev. A* **63**, 044301 (2001).
- [18] D. A. Meyer and N. R. Wallach, Global entanglement in multiparticle systems, *Journal of Mathematical Physics* **43**, 4273 (2002).
- [19] M. Jakob and J. A. Bergou, Complementarity and entanglement in bipartite qudit systems, *Phys. Rev. A* **76**, 052107 (2007).
- [20] E. Rains, Quantum shadow enumerators, *IEEE Transactions on Information Theory* **45**, 2361 (1999).
- [21] A. Higuchi and A. Sudbery, How entangled can two couples get?, *Physics Letters A* **273**, 213 (2000).
- [22] A. J. Scott, Multipartite entanglement, quantum-error-correcting codes, and entangling power of quantum evolutions, *Phys. Rev. A* **69**, 052330 (2004).
- [23] F. Huber, O. Gühne, and J. Siewert, Absolutely maximally entangled states of seven qubits do not exist, *Phys. Rev. Lett.* **118**, 200502 (2017).
- [24] P. Facchi, G. Florio, U. Marzolino, G. Parisi, and S. Pascazio, Multipartite entanglement and frustration, *New Journal of Physics* **12**, 025015 (2010).
- [25] P. Facchi, G. Florio, G. Parisi, and S. Pascazio, Maximally multipartite entangled states, *Phys. Rev. A* **77**,

- 060304 (2008).
- [26] P. Facchi, G. Florio, and S. Pascazio, Probability-density-function characterization of multipartite entanglement, *Phys. Rev. A* **74**, 042331 (2006).
- [27] O. Giraud, Distribution of bipartite entanglement for random pure states, *Journal of Physics A: Mathematical and Theoretical* **40**, 2793 (2007).
- [28] P. Facchi, G. Florio, U. Marzolino, G. Parisi, and S. Pascazio, Statistical mechanics of multipartite entanglement, *Journal of Physics A: Mathematical and Theoretical* **42**, 055304 (2009).
- [29] P. Facchi, Multipartite entanglement in qubit systems, *Atti Accad. Naz. Lincei Cl. Sci. Fis. Mat. Natur.* **20**, 25 (2009).
- [30] P. Facchi, G. Florio, U. Marzolino, G. Parisi, and S. Pascazio, Classical statistical mechanics approach to multipartite entanglement, *Journal of Physics A: Mathematical and Theoretical* **43**, 225303 (2010).
- [31] A. T. Butson, *Proceedings of the American Mathematical Society* **13**, 894 (1962).
- [32] W. Tadej and K. Życzkowski, A concise guide to complex Hadamard matrices, *Open Syst Inf Dyn* **13**, 133–177 (2006).
- [33] M. Rossi, M. Huber, D. Bruß, and C. Macchiavello, Quantum hypergraph states, *New Journal of Physics* **15**, 113022 (2013).
- [34] C. Kruszynska and B. Kraus, Local entanglability and multipartite entanglement, *Phys. Rev. A* **79**, 052304 (2009).
- [35] M. Rossi, D. Bruß, and C. Macchiavello, Hypergraph states in Grover’s quantum search algorithm, *Physica Scripta* **2014**, 014036 (2014).
- [36] C. E. Mora, H. J. Briegel, and B. Kraus, Quantum Kolmogorov complexity and its applications, *International Journal of Quantum Information* **05**, 729 (2007), <https://doi.org/10.1142/S0219749907003171>.
- [37] D. Goyeneche, D. Alsina, J. I. Latorre, A. Riera, and K. Życzkowski, Absolutely maximally entangled states, combinatorial designs, and multiunitary matrices, *Phys. Rev. A* **92**, 032316 (2015).
- [38] D. Goyeneche, Z. Raissi, S. Di Martino, and K. Życzkowski, Entanglement and quantum combinatorial designs, *Phys. Rev. A* **97**, 062326 (2018).
- [39] J. Paczos, M. Wierziński, G. Rajchel-Mieldzióć, A. Burchardt, and K. Życzkowski, Genuinely quantum solutions of the game sudoku and their cardinality, *Phys. Rev. A* **104**, 042423 (2021).
- [40] S. A. Rather, A. Burchardt, W. Bruzda, G. Rajchel-Mieldzióć, A. Lakshminarayan, and K. Życzkowski, Thirty-six entangled officers of Euler: Quantum solution to a classically impossible problem, *Phys. Rev. Lett.* **128**, 080507 (2022).
- [41] K. Życzkowski, W. Bruzda, G. Rajchel-Mieldzióć, A. Burchardt, S. Ahmad Rather, and A. Lakshminarayan, $9 \times 4 = 6 \times 6$: Understanding the quantum solution to Euler’s problem of 36 officers, *Journal of Physics: Conference Series* **2448**, 012003 (2023).
- [42] K. Życzkowski and H.-J. Sommers, Induced measures in the space of mixed quantum states, *Journal of Physics A: Mathematical and General* **34**, 7111 (2001).
- [43] E. Lubkin, Entropy of an n-system from its correlation with a k-reservoir, *Journal of Mathematical Physics* **19**, 1028 (1978).
- [44] S. Lloyd and H. Pagels, Complexity as thermodynamic depth, *Annals of Physics* **188**, 186 (1988).
- [45] D. N. Page, Average entropy of a subsystem, *Phys. Rev. Lett.* **71**, 1291 (1993).
- [46] A. J. Scott and C. M. Caves, Entangling power of the quantum baker’s map, *Journal of Physics A: Mathematical and General* **36**, 9553 (2003).
- [47] P. Facchi, G. Florio, and S. Pascazio, Characterizing and measuring multipartite entanglement, *International Journal of Quantum Information* **05**, 97 (2007).
- [48] G. Cenedese, M. Bondani, D. Rosa, and G. Benenti, Generation of pseudo-random quantum states on actual quantum processors, *Entropy* **25** (2023).
- [49] I. Bengtsson and K. Życzkowski, *Geometry of Quantum States: An Introduction to Quantum Entanglement*, 2nd ed. (Cambridge University Press, 2017).
- [50] Y. Zhou and A. Hamma, Entanglement of random hypergraph states, *Phys. Rev. A* **106**, 012410 (2022).
- [51] D. Bruß and C. Macchiavello, Multipartite entanglement in quantum algorithms, *Phys. Rev. A* **83**, 052313 (2011).
- [52] Y. Liu, W.-J. Li, X. Zhang, M. Lewenstein, G. Su, and S.-J. Ran, Entanglement-based feature extraction by tensor network machine learning, *Frontiers in Applied Mathematics and Statistics* **7**, 10.3389/fams.2021.716044 (2021).
- [53] G. C. Santra, S. S. Roy, D. J. Egger, and P. Hauke, Genuine multipartite entanglement in quantum optimization, *Phys. Rev. A* **111**, 022434 (2025).
- [54] X. Yuan, J. Sun, J. Liu, Q. Zhao, and Y. Zhou, Quantum simulation with hybrid tensor networks, *Phys. Rev. Lett.* **127**, 040501 (2021).
- [55] J. Schuhmacher, M. Ballarin, A. Baiardi, G. Magnifico, F. Tacchino, S. Montangero, and I. Tavernelli, Hybrid tree tensor networks for quantum simulation, *PRX Quantum* **6**, 010320 (2025).
- [56] X.-D. Cai, D. Wu, Z.-E. Su, M.-C. Chen, X.-L. Wang, L. Li, N.-L. Liu, C.-Y. Lu, and J.-W. Pan, Entanglement-based machine learning on a quantum computer, *Phys. Rev. Lett.* **114**, 110504 (2015).
- [57] F. El Ayachi and M. El Baz, Enhancing quantum support vector machines using multipartite entanglement, *Physics Letters A* **551**, 130666 (2025).
- [58] Z. Raissi, C. Gogolin, A. Riera, and A. Acín, Optimal quantum error correcting codes from absolutely maximally entangled states, *Journal of Physics A: Mathematical and Theoretical* **51**, 075301 (2018).
- [59] P. Mazurek, M. Farkas, A. Grudka, M. Horodecki, and M. Studziński, Quantum error-correction codes and absolutely maximally entangled states, *Phys. Rev. A* **101**, 042305 (2020).
- [60] ReCaS-Bari, <https://www.recas-bari.it/>.
- [61] F. Mezzadri, How to generate random matrices from the classical compact groups, *Notices of the American Mathematical Society* **54**, 592 (2007).